Proceedings of the 2016 11th International Pipeline Conference
IPC2016
September 26 - September 30, 2016, Calgary, Alberta, Canada

IPC2016-64061

NUMERICAL SIMULATIONS OF BURST OF CORRODED PIPES WITH THERMALLY INDUCED COMPRESSIVE AXIAL STRAIN

Sérgio B. Cunha [(1)]
TRANSPETRO
Rio de Janeiro, RJ, Brazil

Mauricio Pacheco
ESSS
Rio de Janeiro, RJ, Brazil

Amanda B. da Silva
ESSS
Rio de Janeiro, RJ, Brazil

KEYWORDS
Compressive Axial Strain, Burst, Instability.

ABSTRACT
Some onshore pipelines conduct fluids that are too viscous to be conducted at ambient temperature; they must be heated to enable efficient pumping and flow. These pipelines present a failure rate that is many times larger than those that operate at ambient temperature. The prevailing failure mode for these pipelines is external corrosion: the external thermal insulating coating can give rise to a very severe corrosion process.

Although corrosion is a significant threat for pipelines that operate with heated fluids, the available corrosion assessment methodologies might not be appropriate for this situation. Several studies have been conducted considering a pipeline with a corrosion flaw with axial stress (or load) plus pressure. But a heated pipeline with axial restraint – as caused by the soil friction in a buried pipeline – imparts a compressive axial strain, not a stress. Although in the elastic regimen the thermally induced axial strain generates significant axial stress, it can be expected some level of decrease in the axial stress after yielding, due to the large reduction in the material stiffness and the increase in Poison's ratio. Since localized yield in the flaws is allowed in the assessment of a corrosion flaw, it seems too conservative to use the elastic axial stress in this assessment.

In this article a numerical study of the effects of the temperature in the burst pressure of a pipeline with axial restraint and thermal expansion is presented. Finite element simulations were conducted using actual tensile test curves for two pipeline steel grades, API 5L Gr B and X70. The boundary conditions assumed axial restraint with free radial displacement. The loading comprised an initial heat of the pipe's material and, afterwards, gradual increase of the pressure until burst, assumed to occur by plastic instability. Two diameter to thickness ratio and several flaw geometries were studied.

Initially, the effect of the temperature was evaluated for pipes without defect. Afterwards, numerical simulations of the burst of pipe sections with volumetric flaws of various depth and length were conducted. For both the cases of pipes with and without defect, the simulations were carried out comparing the cases of heated and not heated pipes.

It was found that although the thermal effect causes a large compressive axial stress in the elastic regimen, this stress is almost completely relaxed after yielding. No effect of the temperature in the burst pressure was observed in the numerical simulations.

INTRODUCTION
Some onshore pipelines conduct fluids that are too viscous to be conducted at ambient temperature; they must be heated to enable efficient pumping and flow. Both in Europe [1] and in Brazil [2], pipelines in such conditions present a failure rate many times larger than those that operate at ambient temperature. The prevailing failure mode for these pipelines is external corrosion: the external thermal insulating coating can give rise to a very severe corrosion process.

Although corrosion is a significant threat for pipelines that operate with heated fluids, the available corrosion assessment methodologies might not be appropriate for this situation. The combination of the thermal dilation with the axial restraint imposed by the soil friction generates an axial compressive strain. Most assessment methodologies are not prepared to cope with this situation.

Several studies [3] – [10] have been conducted considering a pipeline with a corrosion flaw submitted to axial stress (or load) in addition to pressure. DNV's Corroded Pipeline Assessment Standard [11] provides a guideline for evaluation of a pipeline with axial load, and recommends the use of the compressive elastic axial stress in the assessment of heated, axially restrained pipelines.

The previous methodologies seem too restrictive to the assessment of a buried and heated pipeline. By heating an axially restrained pipeline, a compressive axial strain is generated. In the elastic regimen this axial strain causes significant axial stress. But some level of decrease in the axial stress can be expected after yielding, due to the large reduction

[(1)] Currently at Rio de Janeiro State University (UERJ), Mechanical Engineering Department.

in the material stiffness and the increase in Poison's ratio. Since localized yield in the flaws must be allowed in any corrosion assessment methodology, it seems too conservative to use the elastic axial stress in the flaw assessment. Smith and Waldhart [7] realized that a strain based assessment would be more realistic, but did not develop their proposal into a methodology.

In this article a numerical study of the effects of the temperature in the burst pressure of a pipeline with axial restraint and thermal load is presented. Initially, pipes without defect were studied. Afterwards, simulations for pipes with volumetric flaws were carried out.

It was found that although the thermal effect causes a large compressive axial stress in the elastic regimen, this stress is almost completely relaxed after yielding. No effect of the temperature in the burst pressure was observed in the numerical simulations.

NOMENCLATURE

d	flaw depth
n	hardening exponent
t	pipe wall thickness
w	flaw half-width
D	pipe external diameter
E	elasticity (Young's) modulus
É	secant stiffness modulus
K	plastic stiffness
L	flaw half-length
M	model length
P	pressure
Sy	tensile test yield strength
Su	tensile test ultimate strength
T	temperature
α	coefficient of thermal dilation
ν	Poison's ratio
ε	strain
ε_θ	circumferential strain
$\bar{\varepsilon}$	equivalent strain
σ	stress
$\bar{\sigma}$	von Mises equivalent stress

NUMERICAL METHODOLOGY

The numerical simulations were carried out by finite element method (FEM) carried out using ANSYS Mechanical 16.0© [12]. The simulations comprised pipes with volumetric flaws and pipes without flaws.

The boundary conditions assumed axial restraint with free radial displacement. The loading comprised an initial heat of the pipe's material and, afterwards, gradual increase of the pressure until burst.

The simulations were performed with solid elements with quadratic interpolation. Three elements composed the wall thickness. A mesh sensibility analysis was carried out, indicating that an element size of 22 mm was adequate. Figure 1 illustrates the mesh for used for simulating a pipe without flaw and Figure 2 shows a FEM mesh of the pipe with a volumetric flaw.

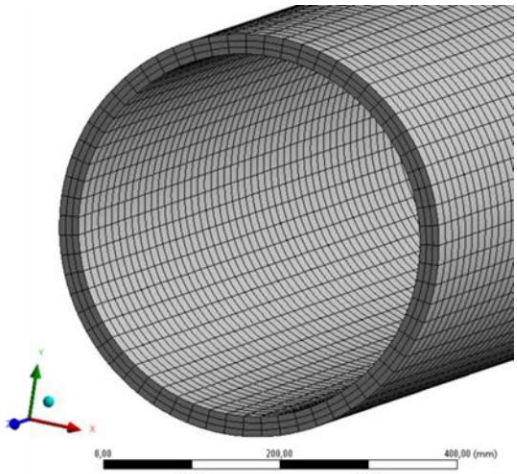

Figure 1: FEM MESH – PIPE without FLAW.

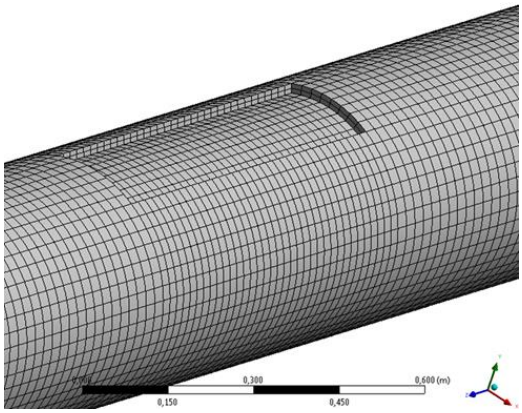

Figure 2: FEM MESH – PIPE with FLAW.

The pipe burst was modelled using Considère's [13] instability principle. In order to determine instability pressure, it is necessary to use a numerical methodology capable of evaluating the system behavior close to the instability, and thus safely determine the inflexion point in the pressure-displacement curve.

The most appropriate methodology for instability analysis is the Load Control approach, which incrementally increases the load. However, this approach restricts the numerical method employed, since at the inflexion point of the load-displacement curve, the stiffness matrix has a determinant equal to zero, which causes potential divergence.

This characteristic prevents the problem to be solved with the Newton-Raphson method, the most common iterative method for FEM. In fact, it is often assumed that the divergence load in such an analysis is equal to the instability load.

To circumvent this issue, the Arc-Length method, initially developed by Riks [14], was employed. The Arc-Length method introduces a load factor, λ ($-1 < \lambda < 1$), to the Newton-Raphson equations. The load factor enforces a spherical convergence path, enabling a null or negative stiffness matrix, as shown in Figure 3.

.

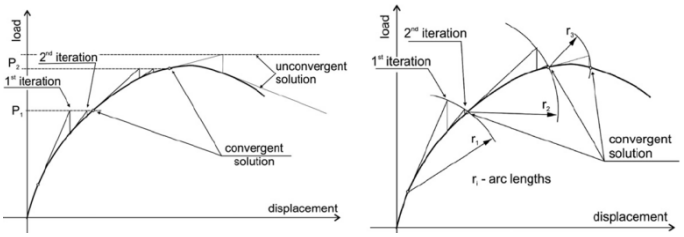

(a) (b)

Figure 3: Graphic representation of the Newton-Raphson (a) and the Arc-Length (b) load paths.

The ANSYS software employs a variation of the Riks method, proposed by Chrisfield [15]. The load balance is controlled by Equation (1), where $[K_i^t]$ is the stiffness matrix for each iteration, $\{F^a\}$ is the total load applied in each sub step, and $\{R_i\}$ is the internal load vector for the nodes.

$$[K_i^t]\{\Delta u_i\} = \Delta\lambda\{F^a\} - \{R_i\} \quad (1)$$

The full mathematical details of this algorithm may be found in the ANSYS manual [12].

FINITE ELEMENT SIMULATIONS

Two actual pipeline steel curves, API 5L Gr B and X70, were employed in the numerical simulations. The tensile test data was transformed into real stress and logarithmic strain up to Su. The material behavior beyond Su was modeled by Ludwig's power law Equation (2).

$$\bar{\sigma} = K\bar{\varepsilon}^n \quad (2)$$

Figure 4 and Figure 5 present the Gr B and X70 tensile curves: the nominal stress vs engineering strain, the real stress (up to Su) vs. logarithmic strain and Ludwig's law vs. logarithmic strain, where the values for K and n were determined using the tensile test data. Table 1 introduces the material parameters found at the tensile test for both steel grades.

Table 1: Material properties.

	X 70	Gr B
E (Gpa)	215	205.9
ν	0.3	0.3
Su (MPa)	713.9	440.8
Sy (MPa)	500.1	335.1
K (MPa)	945.5	689.1
n	0.079	0.157

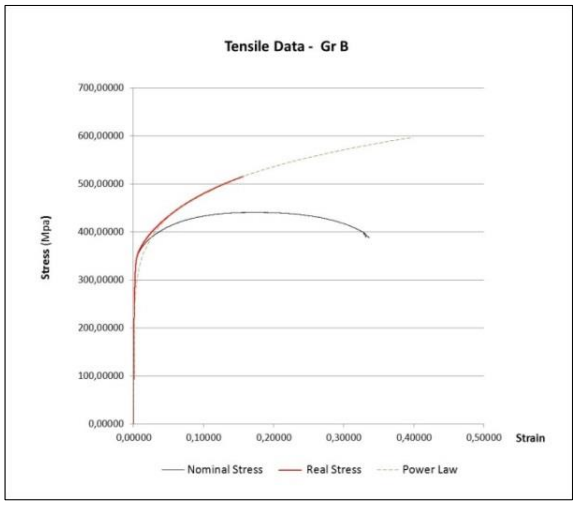

Figure 4: API 5L Gr B TENSILE DATA.

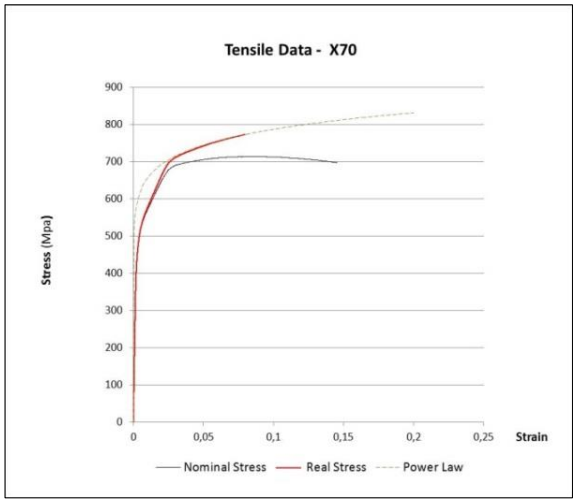

Figure 5: API 5L X70 TENSILE DATA.

Initially, 12 simulations were carried out for pipe sections without flaw, comparing the cases for 0, 70 and 120°C of difference between the temperature of pipe installation and operation. Table 2 presents the parameters utilized for these simulations.

Table 2: Simulation parameters for pipes w/o flaw.

Parameter	Symbol	Value	Unit
external diameter	D	18 – 457.2	inch - mm
slenderness ratio	D/t	20 and 60	-
model length	M	2286	mm
temperature	T	0, 70 and 120	°C
thermal dilation coeff.	α	1.1 x10^{-6}	°C
material	Steel	Gr B and X 70	API 5L

Afterwards, 36 numerical simulations were conducted, for pipe sections with volumetric flaws of various depth and length, comparing the cases of 0 and 80° C temperature differential. Table 3 presents the parameters utilized for the simulations of pipes with flaw, while Figure 6 shows the nomenclature employed for defining the flaws.

Table 3: Simulation parameters for pipes with flaw.

Parameter	Symbol	Value	Unit
external diameter	D	18 – 457.2	inch - mm
slenderness ratio	D/t	60 and 20	-
flaw depth	d/t	0.25; 0.50; 0.75	-
flaw length	L/D	0.1; 0.3; 1.5	-
flaw half width	w	π/8	rd
model length	M	2286	mm
temperature	T	0, 80°C	°C
thermal dilation coeff.	α	1.1 x10^{-6}	°C
material	Steel	Gr B and X 70	API 5L

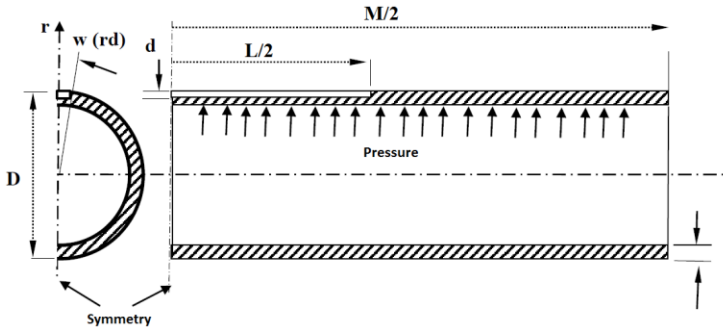

Figure 6: Nomenclature for flaw definition.

SIMULATIONS RESULTS AND DISCUSSION

The numerical simulations do not indicate any decrease in the capability of a pipe to withstand pressure to rupture due to the axial compression caused by the thermal dilation of a pipe with complete axial restraint.

The burst pressure obtained by simulation of plastic instability of pipes without defect, and their associated circumferential strain, are presented in Table 4. The simulation results indicate that the temperature does change the strain at instability, but the burst pressure remains virtually unchanged.

Table 4: Simulation results for pipes w/o flaw.

		ΔT (°C)					
		0		70		120	
D/t	Steel	P (MPa)	ε_θ	P (MPa)	ε_θ	P (MPa)	ε_θ
20	Gr B	49.03	0.0786	49.04	0.0827	49.068	0.0801
	X 70	82.52	0.0498	82.55	0.0507	82.564	0.0462
60	Gr B	15.75	0.0818	15.75	0.0815	15.76	0.0851
	X 70	26.52	0.0488	26.53	0.0509	26.54	0.0504

The axial stress for an axially restrained pipe with a temperature increase and internal pressure is given by Equation (3).

$$\sigma_a = \nu\sigma_\theta - \acute{E}\alpha\Delta T \quad (3)$$

In the elastic region, the secant modulus is identical to the Young's modulus and Poisson's ratio is about 0.3. After yielding deformation occurs at constant volume, thus the Poisson's ratio value is 0.5. Furthermore, the plastic secant stiffness is much smaller than Young's modulus.

Figure 7 to 14 show the von Mises and axial stress for the three different temperatures, for the cases studied. In the elastic regimen there is a noticeable difference among the three temperatures. But after yielding, the three cases present the same behavior. Figure 11 to Figure 14 present the axial stress. It can be seen that, as pressure increases, the initially compressive axial stress becomes actually tractive and no difference among the axial stress at the three temperatures can be observed at pressures near burst.

Table 5 and Table 6 present the instability pressure and the circumferential strain in the middle of the flaw, for Gr B and X70 steel grades.

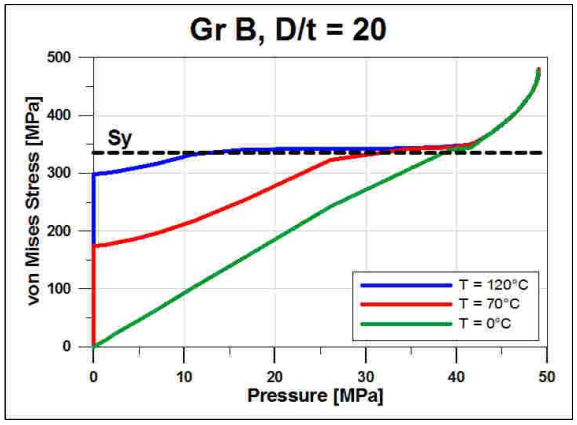

Figure 7: von Mises Stress vs. Pressure Gr B D/t 20.

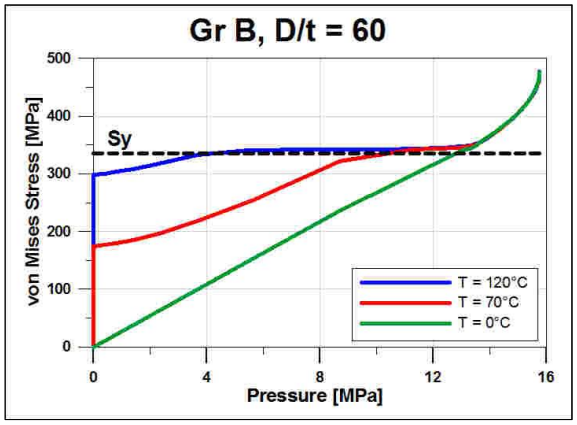

Figure 8: von Mises Stress vs. Pressure Gr B D/t 60.

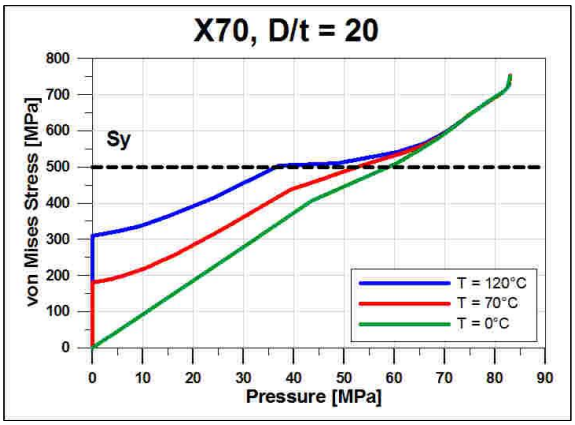

Figure 9: von Mises Stress vs. Pressure X70 D/t 20.

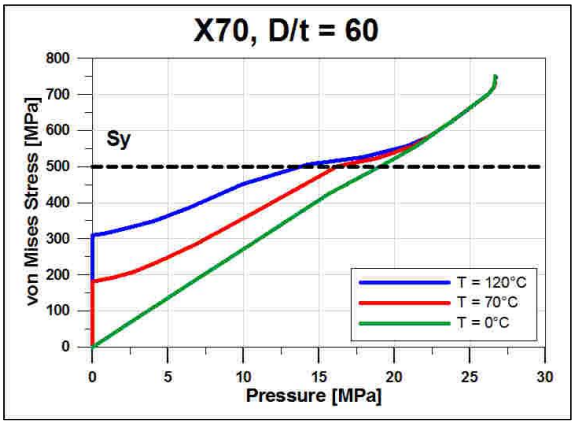

Figure 10: von Mises Stress vs. Pressure X70 D/t 20.

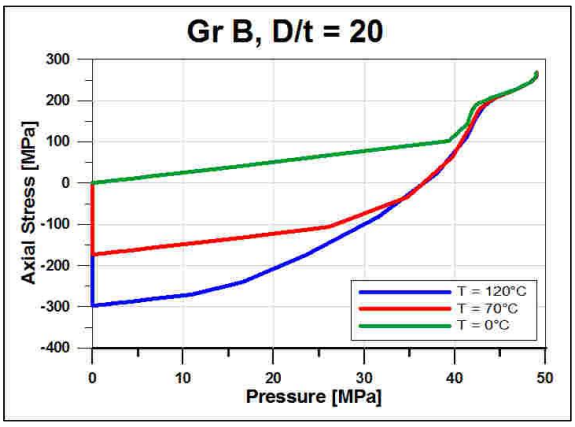

Figure 11: Axial Stress vs. Pressure Gr B D/t 20.

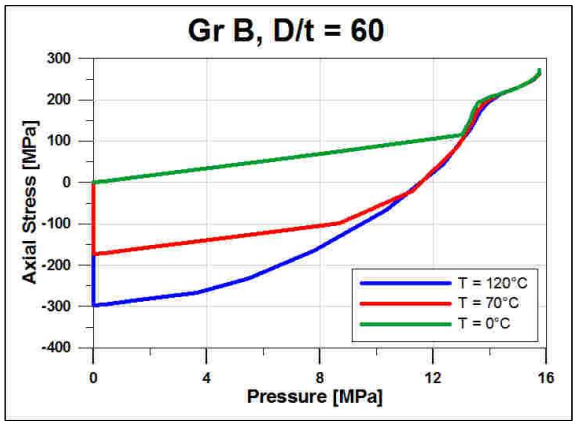

Figure 12: Axial Stress vs. Pressure Gr B D/t 60.

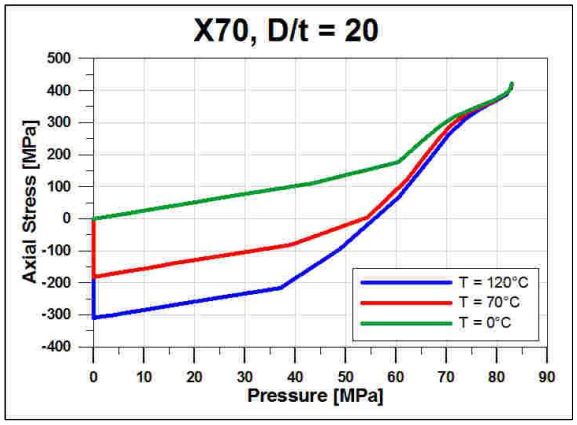

Figure 13: Axial Stress vs. Pressure X70 D/t 20.

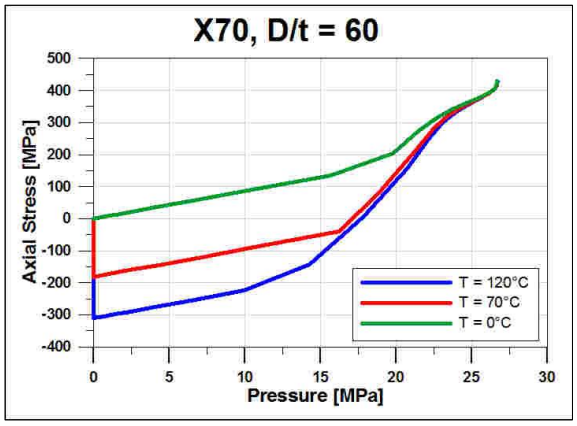

Figure 14: Axial Stress vs. Pressure X70 D/t 60.

Table 5: Simulation Results for Gr B Pipes with Flaw.

	Flaw Geometry		ΔT (°C) 0		80	
D/t	d/t	L	P (MPa)	ε_θ	P (MPa)	ε_θ
20	0.25	0.1 D	48.88	0.138	48.89	0.128
	0.5	0.1 D	48.28	0.169	48.36	0.161
	0.75	0.1 D	45.88	0.197	46.13	0.197
	0.25	0.3 D	45.76	0.128	47.85	0.166
	0.5	0.3 D	42.81	0.150	43.24	0.137
	0.75	0.3 D	34.94	0.207	34.91	0.208
	0.25	1.5 D	42.01	0.091	42.08	0.075
	0.5	1.5 D	30.01	0.092	29.42	0.082
	0.75	1.5 D	16.77	0.091	16.13	0.082
60	0.25	0.1 D	15.82	0.122	15.83	0.119
	0.5	0.1 D	15.6	0.138	15.63	0.132
	0.75	0.1 D	14.73	0.172	14.82	0.163
	0.25	0.3 D	15.32	0.098	15.36	0.097
	0.5	0.3 D	13.67	0.125	13.76	0.109
	0.75	0.3 D	10.68	0.199	10.6	0.187
	0.25	1.5 D	13.52	0.068	13.5	0.056
	0.5	1.5 D	9.39	0.077	9.17	0.065
	0.75	1.5 D	4.98	0.089	4.76	0.079

Table 6: Simulation Results for X70 Pipes with Flaw.

	Flaw Geometry		ΔT (°C) 0		80	
D/t	d/t	L	P (MPa)	ε_θ	P (MPa)	ε_θ
20	0.25	0.1 D	82.66	0.082	82.69	0.082
	0.5	0.1 D	80.78	0.110	80.78	0.104
	0.75	0.1 D	75.6	0.167	75.79	0.161
	0.25	0.3 D	79.14	0.079	79.25	0.079
	0.5	0.3 D	67.86	0.114	68.03	0.110
	0.75	0.3 D	54.89	0.192	54.34	0.178
	0.25	1.5 D	67.41	0.056	67.24	0.049
	0.5	1.5 D	46.87	0.055	46	0.049
	0.75	1.5 D	25.36	0.054	24.56	0.047
60	0.25	0.1 D	26.56	0.067	26.56	0.068
	0.5	0.1 D	25.72	0.079	25.76	0.083
	0.75	0.1 D	23.74	0.132	23.87	0.135
	0.25	0.3 D	24.95	0.064	24.95	0.063
	0.5	0.3 D	21	0.097	21.06	0.088
	0.75	0.3 D	16.05	0.173	15.82	0.166
	0.25	1.5 D	21.45	0.041	21.43	0.036
	0.5	1.5 D	14.57	0.044	14.35	0.036
	0.75	1.5 D	7.49	0.047	7.28	0.039

The instability pressure is virtually the same for the two temperatures for all geometries simulated, for both Gr B and X70 steel grades. The cases at higher temperatures presented less circumferential strain at instability than the cases at ambient temperature.

Figure 15 and Figure 16 show the von Mises stress in the middle of the flaw, comparing the two different temperatures studied, for different flaw depths. It may be observed that, although the stress is very dissimilar before yielding, the temperature influence almost disappears in the plastic region.

Figure 17 and Figure 18 compare the axial stress in the center of the flaw for the two temperatures. As was observed in the simulation of the pipe without flaw, although stress is initially compressive, it becomes tensile after yielding as pressure is increased.

A similar behavior was observed for all cases studied.

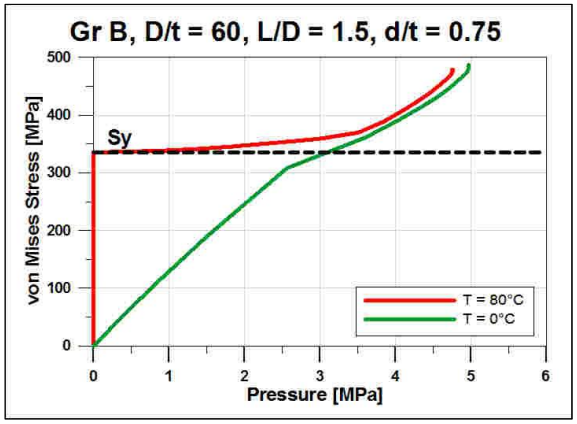

(a)

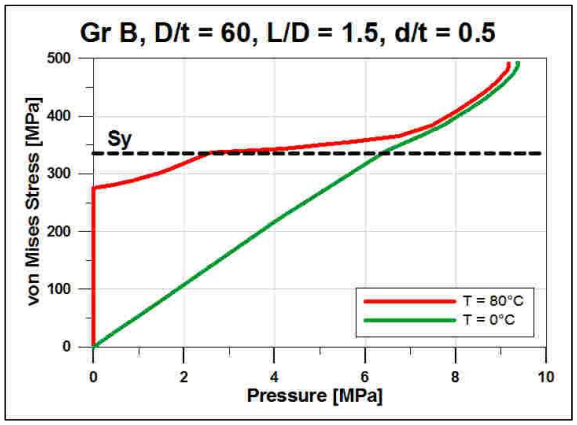

(b)

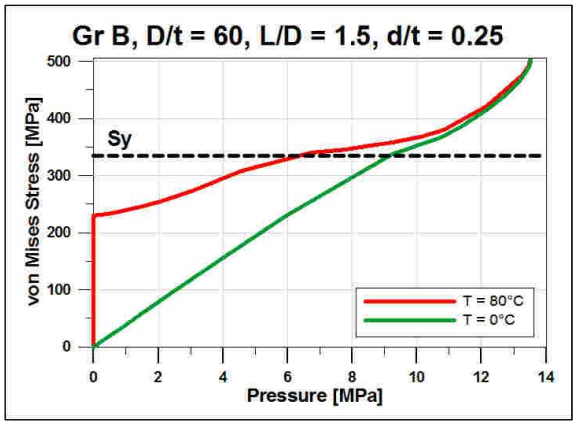

(c)

Figure 15: von Mises Stress vs. Pressure for Gr B, for flaw depth of (a) d/t = 0.75; (b) d/t = 0.5; and (c) d/t = 0.25.

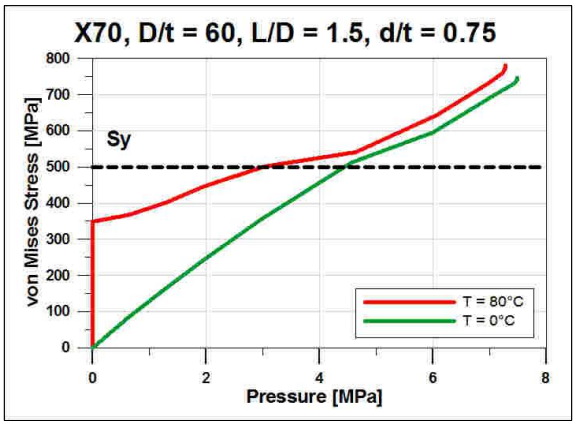

(a)

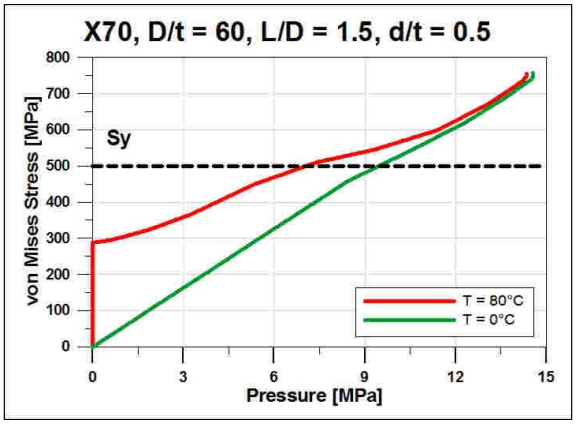

(b)

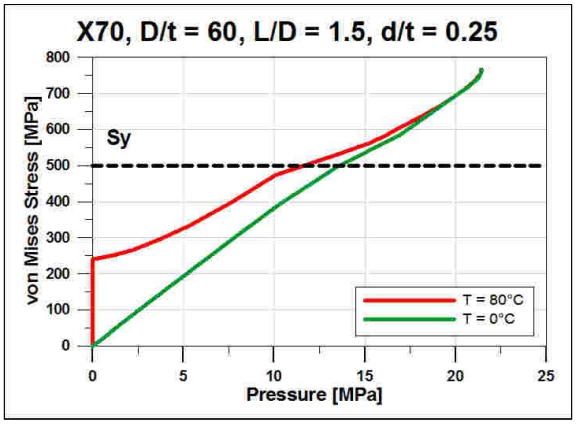

(c)

Figure 16: von Mises Stress vs. Pressure for X70, for flaw depth of (a) d/t = 0.75; (b) d/t = 0.5; and (c) d/t = 0.25.

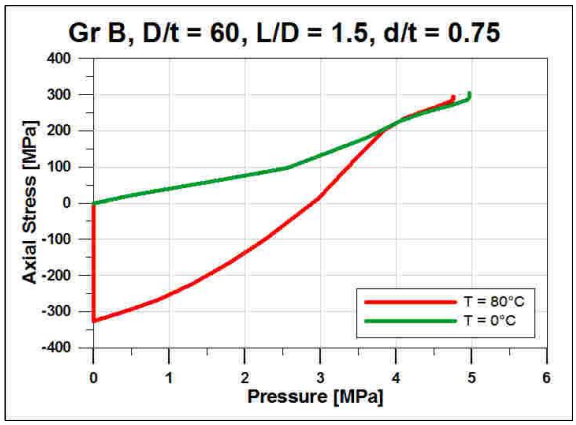

(a)

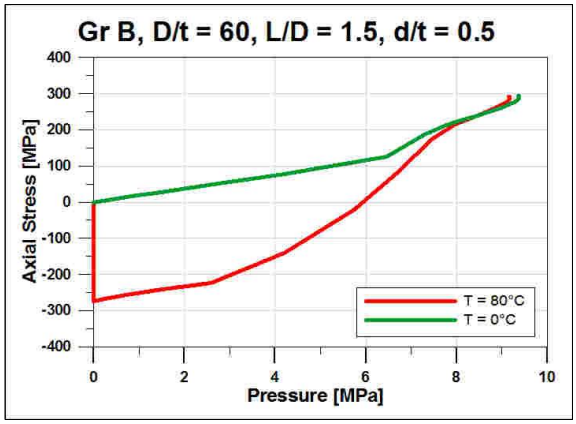

(b)

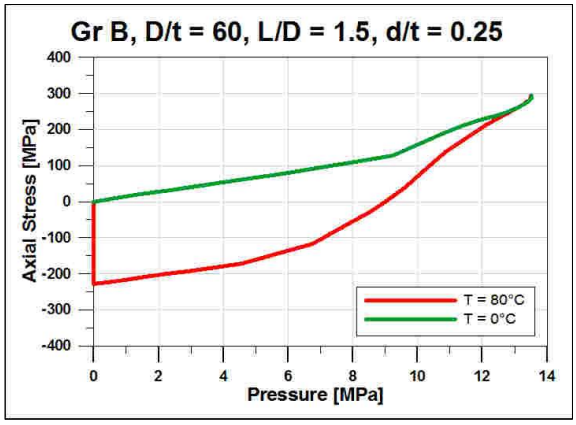

(c)

Figure 17: Axial Stress vs. Pressure for Gr B, for flaw depth of (a) d/t = 0.75; (b) d/t = 0.5; and (c) d/t = 0.25.

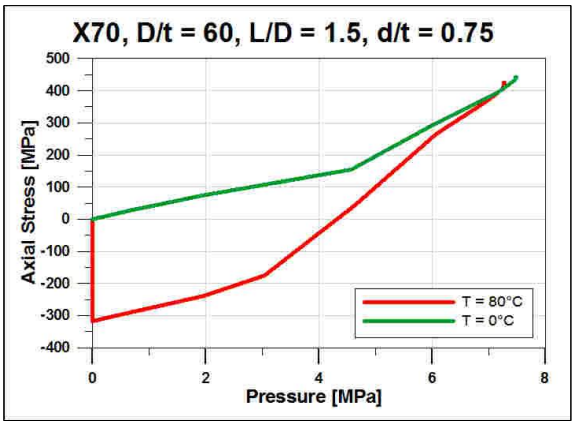

(a)

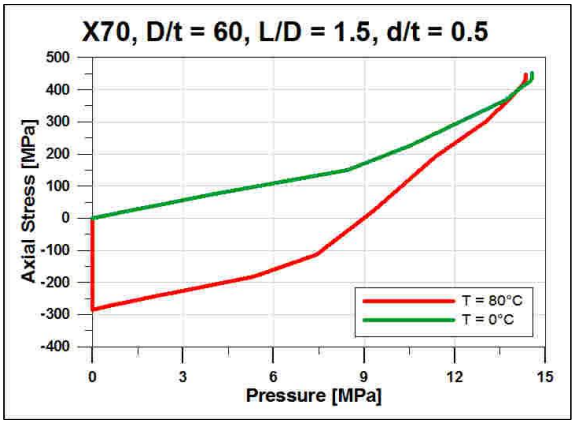

(b)

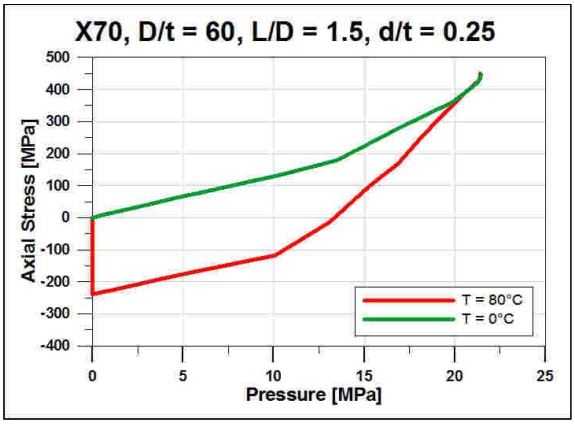

(c)

Figure 18: Axial Stress vs. Pressure for X70, for flaw depth of (a) d/t = 0.75; (b) d/t = 0.5; and (c) d/t = 0.25.

CONCLUSIONS

A series of numerical simulations of burst of pipe sections were conducted by the finite elements method, analyzing the effect of a compressive axial strain generated by thermal dilation of an axially constrained pipe. The simulations replicated the condition of a buried pipeline conducting heated fluids. The simulations comprised two steel grades (Gr B and X 70) and two slenderness ratio (D/t), 20 and 60. Pipes without flaws and pipes with various flaws geometry were studied. The burst was modelled by plastic instability.

The numerical results indicate that an axially restrained heated pipe can withstand the same pressure until burst that a pipe operating at ambient conditions, in the range of temperatures studied.

While in the elastic region the thermal dilation generates a significant compressive stress, after yield the effect of the axial dilation becomes negligible. In all cases, the axial stress was tensile before burst. The decrease in the material stiffness and the increase in Poisson's ratio after yield explains the change in the stresses from the elastic to the plastic regimen.

The FEM simulations indicate that, for the temperatures typical for pumping of heated fluids, the thermally induced axial dilation of an axially restrained pipe does not affect the burst capacity of the pipe, even if a volumetric flaw is present. Experimental confirmation of these results is envisioned.

ACKNOWLEDGMENTS

The authors wish to thank TRANSPETRO and ESSS for supporting this study. The authors also want to express their gratitude to ESSS technical staff for conducting the numerical simulations.

REFERENCES

[1] Davis, P. M., Dubois, J., Gambardella, F., Sanchez-Garcia, E., Uhlig F., (2011). "Performance of European cross-country oil pipelines - Statistical summary of reported spillages in 2010 and since 1971". Report no. 8/11, CONCAWE, http://www.concawe.be.

[2] Cunha, S.., (2012). "Comparison and analysis of pipeline failure statistics". International Pipeline Conference 2012, IPC2012-90186.

[3] Roy S., Grigory S., Smith M., Kanninen M. F., Anderson M., (1997) "Numerical simulations of full scale corroded pipe tests with combined loading ", Journal of Pressure Vessel Technology, November 1997, Vol. 119, p 457-466.

[4] Liu J., Chauhan V., Ng P., Wheat S., Hughes C., (2012). "Remaining strength of corroded pipe under secondary (biaxial) loading ". Pipeline Research Council International PRCI Report L 52307, January 2012.

[5] Benjamin A. C., (2008). "Prediction of the failure pressure of corroded pipelines subjected to a longitudinal compressive force superimposed to the pressure loading". International Pipeline Conference 2008, IPC2008-64089.

[6] Bjornoy O.H., Sigurdsson G., Cramer E., (2000). "Residual strength of corroded pipelines, DNV test results", International Offshore and Polar Engineering Conference, 2000.

[7] Smith M.Q., Waldhart C. J., (2000). “Combined loading tests of large diameter corroded pipelines”. International Pipeline Conference 2000, Vol 2 p. 769-779.

[8] Wang W., Smith M.Q., Popelar C. H., Maple J. A., (1998). “A new rupture model for corroded pipelines under combined loading”. International Pipeline Conference 1998, Vol 1 p 563-572.

[9] Roberts K. A., Pick R. J., (1998). “Correction for longitudinal stress in assessment of corroded line pipe”. International Pipeline Conference 1998, Vol 1 p 553-561.

[10] Smith M.Q., Grigory S. C., (1996). “New procedures for the residual strength assessment of corroded pipe subjected to combined loads”. International Pipeline Conference 1996, Vol 1 p. 387-400.

[11] DNV - Det Norske Veritas. Recommended practice DNV RP-F101 – corroded pipelines, 1999.

[12] ANSYS INC (2015). “ANSYS Mechanical 16.0 - Theory Reference”. Manual.

[13] Considère M, (1885). Mémoires sur l’employ du fer et de l’acier dans les constructions. Annales de Ponts et Chausses; 6(9): p. 574 – 775, 1885.

[14] RIKS E., (1979). “An Incremental Approach to the Solution of Snapping and Buckling Problems”. International Journal of Solids and Structures, 7, p 524-551.

[15] CRISFIELD, M. A. (1981). “A fast incremental/iterative solution procedure that handles snap-through”. Computer and Structures, 1, 1981. p. 55-62.